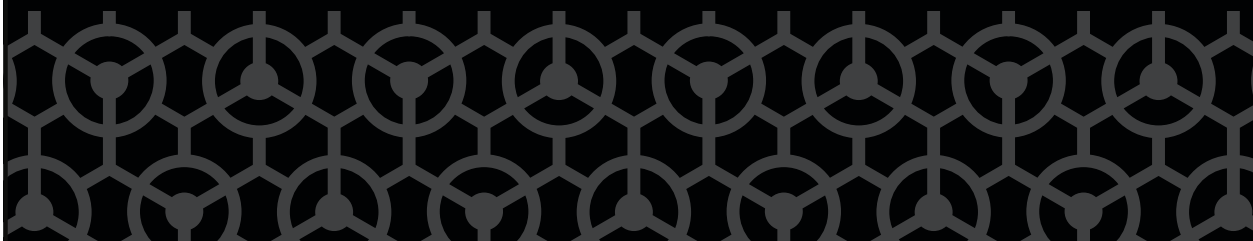




# EurJOC

European Journal of Organic Chemistry

 **Chemistry  
Europe**  
European Chemical  
Societies Publishing



## Accepted Article

**Title:** ortho-Phenylene-based macrocyclic hydrocarbons assembled using olefin metathesis

**Authors:** Viraj C. Kirinda, Briana R. Schrage, Christopher J. Ziegler, and Christopher Scott Hartley

This manuscript has been accepted after peer review and appears as an Accepted Article online prior to editing, proofing, and formal publication of the final Version of Record (VoR). This work is currently citable by using the Digital Object Identifier (DOI) given below. The VoR will be published online in Early View as soon as possible and may be different to this Accepted Article as a result of editing. Readers should obtain the VoR from the journal website shown below when it is published to ensure accuracy of information. The authors are responsible for the content of this Accepted Article.

**To be cited as:** *Eur. J. Org. Chem.* 10.1002/ejoc.202000950

**Link to VoR:** <https://doi.org/10.1002/ejoc.202000950>

WILEY-VCH

# *ortho*-Phenylene-based macrocyclic hydrocarbons assembled using olefin metathesis

Viraj C. Kirinda,<sup>[a]</sup> Briana R. Schrage,<sup>[b]</sup> Christopher J. Ziegler,<sup>[b]</sup> and C. Scott Hartley<sup>\*[a]</sup>

[a] V. C. Kirinda, Dr. C. S. Hartley  
Department of Chemistry & Biochemistry  
Miami University  
Oxford, OH 45056 (USA)  
E-mail: [scott.hartley@miamioh.edu](mailto:scott.hartley@miamioh.edu)  
Homepage: <https://www.hartleygroup.org>

[b] B. R. Schrage, Dr. C. J. Ziegler  
Department of Chemistry  
University of Akron  
Akron, OH 44325 (USA)

Supporting information for this article is given via a link at the end of the document.

**Abstract:** While many foldamer systems reliably fold into well-defined secondary structures, higher order structure remains a challenge. A simple strategy for the organization of folded subunits in space is to link them together within a macrocycle. Previous work has shown that *o*-phenylenes can be co-assembled with rod-shaped linkers into twisted macrocycles, showing an interesting synergy between folding and thermodynamically controlled macrocyclization. In these systems the foldamer units were largely decoupled from each other both conformationally and electronically. Here, we show that hydrocarbon macrocycles, with very short ethylene linkers, can be assembled from *o*-phenylenes using olefin metathesis. Characterization by NMR spectroscopy, X-ray crystallography, and *ab initio* calculations shows that the products are approximately triangular trimer macrocycles with helical *o*-phenylene corners in a heterochiral configuration. Their photophysics are dominated by the 4,4'-diphenylstilbene moieties, the longest conjugated segments, with further conjugation broken by the twisting of the *o*-phenylenes.

## Introduction

The hierarchical structure of biomacromolecules has long inspired chemists to design abiotic *foldamers*, oligomers that adopt well-defined conformations because of noncovalent interactions.<sup>[1–5]</sup> Foldamers exhibiting molecular recognition,<sup>[6–9]</sup> catalysis,<sup>[10,11]</sup> interesting electronic properties,<sup>[12–14]</sup> self-assembly,<sup>[15]</sup> and biological activity<sup>[16–18]</sup> are now known. Ultimately, the goal is to complement biological systems, achieving analogous structural sophistication, and thus function, but using structural motifs with distinct properties. In abiotic foldamer systems, secondary structure, especially the helix, is now fairly well represented. Higher-order structure remains rare, especially in non-peptidic foldamers, even though tertiary and quaternary structure are key to function in analogous biological systems. Only a handful of examples are currently known.<sup>[19–21]</sup>

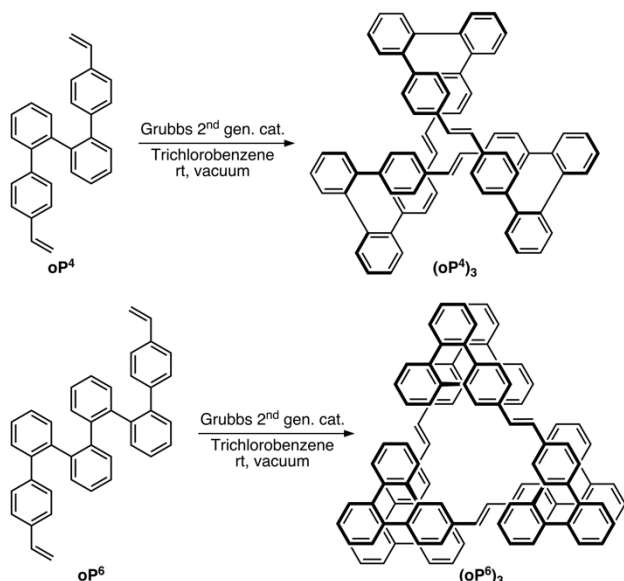
A simple view of higher-order structure is molecular architectures that place folded subunits into well-defined positions. A minimal approach to this challenge is the incorporation of

foldamer moieties within conformationally restricted macrocycles.<sup>[22–24]</sup> To synthesize these targets, folding can be combined with thermodynamically controlled self-assembly, raising questions about how the two concepts together can yield products with emergent structural complexity. For helical foldamers, the products will be twisted macrocycles that combine the features of globally folded macrocycles<sup>[25–31]</sup> with those with conformationally rigid axially chiral subunits.<sup>[32–39]</sup>

Our work has focused on the *ortho*-phenylenes, a simple class of aromatic foldamers.<sup>[40]</sup> They are well-suited to the study of folding combined with self-assembly because of their straightforward conformational behavior, and because of the predictable dependence of their NMR spectra on their geometries, which allows solution-phase folding states to be deduced and quantified. We have previously shown that amine-functionalized *o*-phenylenes can be co-assembled with aldehyde-functionalized rod-shaped linkers.<sup>[22–24]</sup> In these systems, the combination of assembly and folding yields new behavior: for example, because only certain *o*-phenylene conformers will fit within a macrocycle of a particular size, the process of macrocyclization can distort them into folds that are not observed for the unconstrained acyclic oligomers.

In this previous work, assembly occurred very effectively, but the *o*-phenylenes were conformationally and electronically decoupled from each other by their linkers. Questions remain about the tolerance of self-assembly to short restrictive linkers and the possibility of electronic coupling between the *o*-phenylenes. Here, we report the synthesis and characterization of the unsubstituted *ortho*-phenylene macrocycles (**oP<sup>4</sup>**)<sub>3</sub> and (**oP<sup>6</sup>**)<sub>3</sub>, shown in Scheme 1. The macrocycles were assembled using ring closing metathesis (RCM), a well-known and efficient method for the synthesis of macrocycles<sup>[41–46]</sup> and cages.<sup>[47,48]</sup> These conjugated hydrocarbon macrocycles are reminiscent of systems with Möbius  $\pi$  systems,<sup>[36]</sup> including an example prepared by alkyne metathesis,<sup>[49]</sup> which can lead to antiaromaticity. However, the  $\pi$  systems of the two macrocycles reported here are formally continuous (i.e., formally aromatic), and their twisting will attenuate conjugation (especially for (**oP<sup>6</sup>**)<sub>3</sub>).<sup>[50–52]</sup>

## FULL PAPER

Scheme 1. Assembly of macrocycles ( $(oP^4)_3$  and  $(oP^6)_3$ ).

## Results and Discussion

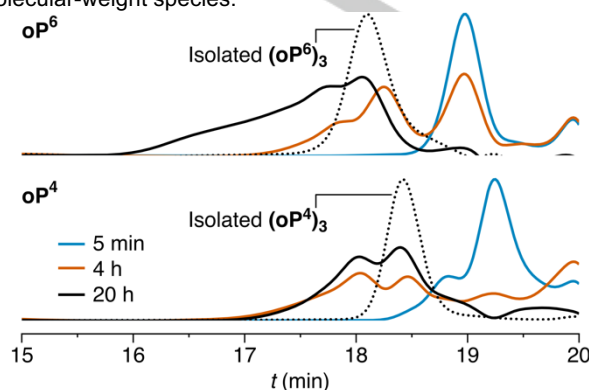
## Synthesis

The macrocycles were synthesized from vinyl-substituted *ortho*-phenylene precursors  $oP^4$  and  $oP^6$ , whose synthesis is described in the Supporting Information. As shown in Scheme 1, these precursors (5 mM) were subjected to macrocyclization by olefin metathesis using the second-generation Grubbs catalyst in 1,2,4-trichlorobenzene at room temperature. The reactions were carried out under vacuum to remove the ethylene byproduct. Aliquots from the reaction mixtures were analyzed by analytical gel permeation chromatography (GPC). Similar product distributions, shown in Figure 1, were obtained in both cases, although there were differences in reactivity. The  $oP^4$  system shows peaks in the chromatograms corresponding to higher molecular weight species after only 5 min, with consumption of most of the starting  $oP^4$  after 4 h. While the total amount of products continues to increase, the relative proportions of higher molecular weight species do not change significantly after the 4 h mark. The reaction of  $oP^6$  proceeds more slowly, with significant starting material still visible for at least 8 h. In both systems, the product distribution is unchanging after 24 h, and no change was observed after adding fresh catalyst and reacting for an additional 24 h.

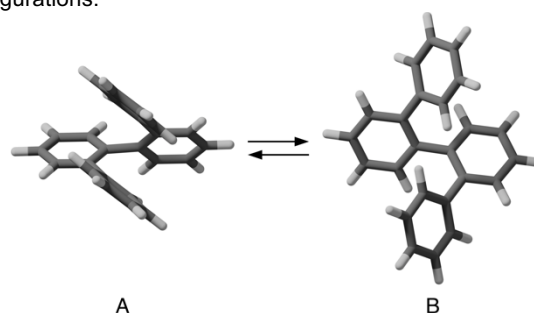
Macrocycles  $(oP^4)_3$  and  $(oP^6)_3$  could be isolated from the reaction mixtures by flash chromatography followed by semi-preparative GPC in 25% and 27% yields, respectively (GPC traces in Figure 1).<sup>[53]</sup> In both cases, mass spectrometry confirmed that the major products were the 3+3 macrocycles. Analysis of fractions corresponding to higher molecular weight species indicated the presence of higher macrocycles, although given the breadth of the peaks it is very likely that acyclic oligomers were also present.<sup>[54]</sup>

As judged by the GPC monitoring experiments, the self-assembly of these macrocycles is much less effective than that of comparable imine-based macrocycles with long linking groups, which typically give product distributions dominated by [3+3] macrocycles.<sup>[22,24]</sup> This is not so surprising given the very short

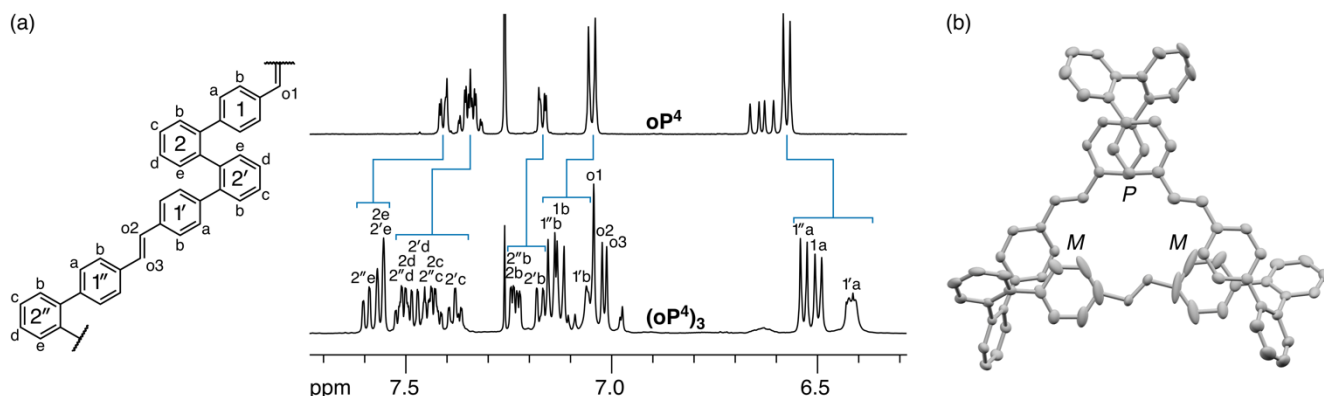
ethylenic linkers of the olefin systems. Increased steric congestion could lead to either kinetic trapping or less-efficient self-assembly because of strain. To test whether the product distributions in Figure 1 represent equilibrium, we carried out experiments where the isolated macrocycles were treated with Grubbs catalyst and allowed to react for 24 h (i.e., to see whether the same product distributions would be obtained when starting with the macrocycles). Unfortunately, the results were inconclusive as the macrocycles simply decomposed to lower-molecular-weight species.

Figure 1. Monitoring of the macrocyclization of  $oP^4$  and  $oP^6$ .Structural analysis of  $(oP^4)_3$ 

The structures of the macrocycles can be understood in the context of the acyclic *o*-phenylenes. As shown in Figure 2, an *o*-phenylene tetramer will rapidly interconvert, via rotation about the central biaryl bond, between a “closed” conformer “A”, which is stabilized by a single aromatic stacking interaction, and an extended “open” conformer “B”. In chloroform, aromatic stacking is not strong enough to completely bias the system toward the folded state. The fit of an *o*-phenylene within a quasi-triangular [3+3] macrocycle can be quantified through the bite angle ( $\beta$ ) made by the terminal positions of the oligomer (i.e., the angle between the vectors passing through the points of attachment at the oligomer termini, brought to a common origin).<sup>[55]</sup> In the A state  $\beta \approx 70^\circ$ , whereas in the B state  $\beta \approx 120^\circ$  for an *o*-phenylene tetramer. Thus, as we have previously shown, only the A state fits within a triangular macrocycle (which requires  $\beta \approx 60^\circ$ ) and macrocyclization induces folding.<sup>[22]</sup> For  $(oP^4)_3$ , we therefore expect a roughly triangular macrocycle with three twisted *o*-phenylene corners. This can exist, in principle, in either homochiral (*PPP* or *MMM*) or heterochiral (*PPM* or *MPP*) configurations.

Figure 2. Conformers of tetra(*o*-phenylene). The enantiomers of these conformers will of course also be present and equally populated.

## FULL PAPER



**Figure 3.** Characterization of  $(\text{oP}^4)_3$  by (a) NMR spectroscopy ( $\text{oP}^4$  top and  $(\text{oP}^4)_3$  bottom,  $\text{CDCl}_3$ , 500 MHz, rt) and (b) X-ray crystallography.

Like other *o*-phenylenes, considerable structural information can be obtained through analysis of the NMR spectra of the macrocycles, particularly when compared to acyclic analogues (i.e.,  $\text{oP}^4$  and  $\text{oP}^6$ ).<sup>[22,24,40]</sup> The spectrum of precursor  $\text{oP}^4$ , shown in Figure 3a, is a good match to that of the parent tetra(*o*-phenylene),<sup>[51]</sup> confirming that it does behave according to Figure 2, with rapid exchange on the NMR time scale. In contrast, the spectrum of cyclized  $(\text{oP}^4)_3$  is complex. Through COSY, HSQC, HMBC, and NOESY/EXSY experiments, it was possible to fully assign the spectrum (Figure 3 and Supporting Information). All of the proton signals in the spectrum are split into three (e.g., protons 1a, 1'a, 1''a), indicating that  $(\text{oP}^4)_3$  has only twofold symmetry in solution. We therefore conclude that it adopts the heterochiral  $C_2$ -symmetric geometry, and not the higher-symmetry homochiral,  $D_3$ -symmetric configuration. Comparing analogous protons between macrocyclic  $(\text{oP}^4)_3$  and acyclic  $\text{oP}^4$ , there are significant differences in chemical shifts (indicated in Figure 3), suggesting a change in conformational distribution for the *o*-phenylene moieties. In particular, the upfield shifts of protons 1a and downfield shifts of protons 2e indicate that, in the macrocycle, the *o*-phenylenes favor the compact A conformer as the nuclei move into and away from the shielding zones of nearby aromatic rings, respectively.<sup>[22]</sup>

We were able to grow X-ray-quality crystals of both  $(\text{oP}^4)_3$ , with the structure shown in Figure 3b, and  $\text{oP}^4$  (Supporting Information).<sup>[56]</sup> The crystal structure confirms the heterochiral configuration deduced from the  $^1\text{H}$  NMR analysis of the bulk solution; a freshly dissolved crystal shows an identical spectrum. Comparison of the two structures shows that the *o*-phenylenes are more tightly folded in the macrocycle, with a mean centroid-to-centroid distance between the terminal rings (1, 1', 1'') of 3.67 Å in  $(\text{oP}^4)_3$ , compared to 4.25 Å in  $\text{oP}^4$ . The central dihedral angle in the *o*-phenylenes is correspondingly reduced to 60° from 62°. This compression of the *o*-phenylene moieties, and the corresponding strain, may at least partly explain the modest efficiency of self-assembly of  $(\text{oP}^4)_3$  compared to systems with longer, more flexible linkers.<sup>[22]</sup>

DFT geometry optimizations at the PCM( $\text{CHCl}_3$ )/B97-D/cc-pVDZ level were performed to further understand the conformational preferences of  $(\text{oP}^4)_3$ . Both heterochiral and homochiral configurations and all four possible orientations of the *trans*-ethynylene groups were explicitly considered (see Supporting Information). Consistent with the NMR and crystallography results, the most-stable heterochiral conformation is predicted to be preferred over the best homochiral conformation

by 4.0 kcal/mol. As was observed in the crystal structures, the DFT calculations predict that the *o*-phenylene moieties are compressed on macrocyclization. However, the effect is much smaller in the calculations (roughly 0.1 Å computationally vs 0.6 Å by crystallography). The difference is in the geometry of  $\text{oP}^4$ , where the centroid-to-centroid distance between terminal rings is underestimated (3.67 Å vs 4.25 Å).

The conformational dynamics of the  $(\text{oP}^4)_3$  system were briefly explored by variable-temperature (VT)  $^1\text{H}$  NMR spectroscopy, with the spectra shown in the Supporting Information. As the temperature was decreased from room temperature to 233 K ( $\text{CDCl}_3$ ), the internal protons of the *o*-phenylenes (rings 2, Figure 3a) did not show significant chemical shift or peak shape changes. In contrast, the signals for the terminal ring protons (rings 1) broadened. This suggests that rotation about the terminal biaryl bonds slows, as has been observed for some acyclic *o*-phenylenes with stronger aromatic stacking interactions.<sup>[57]</sup> Interestingly, the effect is more significant for the protons on rings 1 and 1' (i.e., the *o*-phenylenes with the predominant twist senses). There is relatively little effect as the temperature is increased to 347 K, although there is some sharpening of the signal for proton 1'a, suggesting that its broadened appearance at room temperature results from conformational exchange at an intermediate rate, and that inversion of the *o*-phenylene moieties (e.g.,  $MPP \rightleftharpoons MMP$ ) is slow on the NMR time scale.

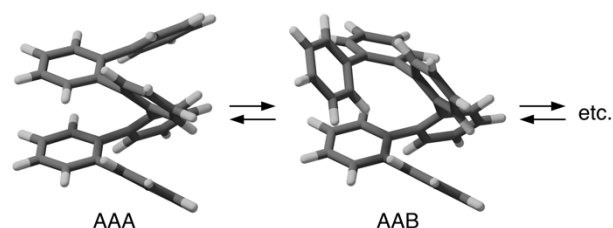


**Figure 4.** Conformations of hexa(*o*-phenylene).

#### Structural analysis of $(\text{oP}^6)_3$

The conformational behavior of *o*-phenylene hexamers is much more complex than that of tetramers. As shown in Figure 4, hexa(*o*-phenylene) can fold into a helix stabilized by three aromatic stacking interactions, called the “AAA” conformer.<sup>[57]</sup> The next most stable conformer is the “AAB” state, which differs in

## FULL PAPER

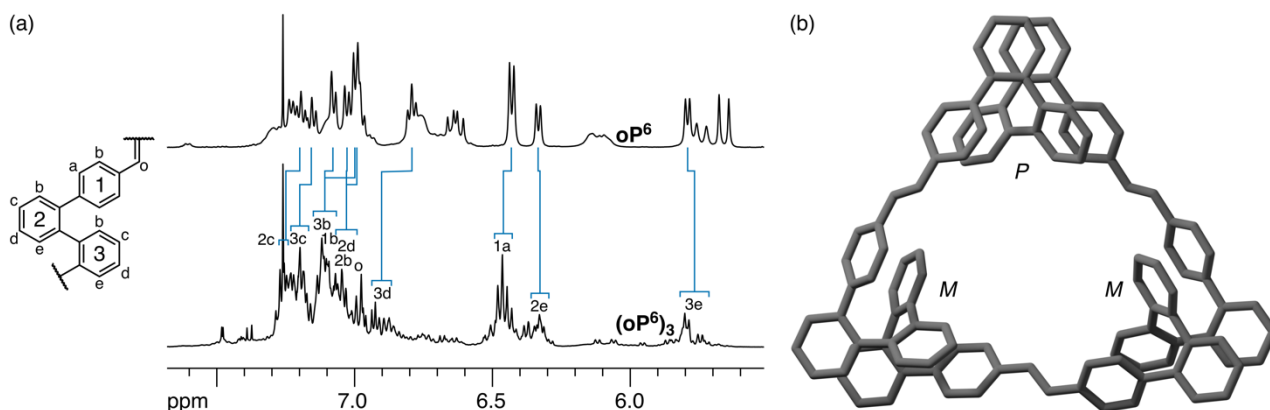


**Figure 5.** (a) Characterization of  $(\text{oP}^6)_3$  by  $^1\text{H}$  NMR spectroscopy ( $\text{oP}^6$  top and  $(\text{oP}^6)_3$  bottom,  $\text{CDCl}_3$ , 500 MHz, rt). (b) Most-stable conformer of  $(\text{oP}^6)_3$ , as determined by DFT optimization at the PCM( $\text{CHCl}_3$ )/B97-D/cc-pVDZ level.

rotation about one of the key biaryl bonds, resulting in the loss of a single stacking interaction. Unlike *o*-phenylene tetramers, interconversion between these more sterically congested conformers is typically slow on the NMR time scale (but fast on the lab time scale). Like the tetramers, the bite angle, and thus the fit within a macrocycle of a given size, is dependent on the conformation, with only the well-folded AAA state compatible with a [3+3] macrocycle ( $\beta \approx 68^\circ$ ).

We were, unfortunately, unable to grow crystals of  $(\text{oP}^6)_3$  suitable for X-ray diffraction, despite many attempts. However, analysis of its NMR spectra and computational optimization provide insight into its structure. For reference, the NMR spectrum of the acyclic  $\text{oP}^6$  is shown in Figure 5a (top). At room temperature, its spectrum is a combination of sharp signals associated with the perfectly folded (helical) conformation and smaller broad peaks corresponding to misfolded states, as verified by EXSY spectroscopy. As is typical for *o*-phenylenes, its  $^1\text{H}$  signals could be assigned through COSY, HSQC, and HMBC spectroscopy; the assigned chemical shifts of the major conformer (see Supporting Information) are a good match to those of the parent hexa(*o*-phenylene).<sup>[51]</sup> By analogy, we conclude that  $\text{oP}^6$  is predominantly well-folded into the AAA state.

The  $^1\text{H}$  NMR spectrum of  $(\text{oP}^6)_3$ , shown in Figure 5a (bottom), is significantly more complex than that of the smaller  $(\text{oP}^4)_3$ . The spectrum shows minor signals corresponding to misfolded *o*-phenylenes, as expected.<sup>[24]</sup> The assignment of these signals to misfolded conformations, as opposed to impurities, is confirmed by EXSY spectroscopy, which shows exchange peaks with signals in the major conformers,<sup>[58]</sup> and VT NMR, which shows coalescence of signals at elevated temperature (see Supporting Information). As before, the chemical shifts of the major conformation were assigned using standard 2D NMR spectra. Unfortunately, while it is clear that there are multiple symmetry-inequivalent protons in the predominant geometry, it was not possible to distinguish specific inequivalent *o*-phenylene moieties. Nevertheless, we can draw several conclusions on the basis of the spectra. First, since separate signals can be identified for many of the protons, it is clear that a  $D_3$ -symmetric homochiral conformer does not predominate. Second, since the signals for each proton do tend to be clustered together within roughly 0.1 ppm, the *o*-phenylenes must favor a single twofold-symmetric geometry as opposed to a mixture of distinct folding states. Third, the chemical shift differences for analogous protons between

$(\text{oP}^6)_3$  and  $\text{oP}^6$  are small ( $<0.2$  ppm); confirming that the *o*-phenylenes remain similarly folded (were that not the case, many proton signals would shift by  $>1$  ppm<sup>[24]</sup>). We cannot, unfortunately, determine whether there is a greater bias toward the AAA conformation in  $(\text{oP}^6)_3$  over  $\text{oP}^6$ , as had been observed in analogous systems,<sup>[24]</sup> using the available data.

At elevated temperatures (343 K), the  $^1\text{H}$  NMR signals of  $(\text{oP}^6)_3$  broaden and coalesce, indicating significant conformational flexibility. Relatively little change in the spectrum is observed as the temperature is decreased, consistent with the oligomers already being in a slow regime for conformational exchange at room temperature.

Candidate geometries of  $(\text{oP}^6)_3$  were optimized at the PCM( $\text{CHCl}_3$ )/B97-D/cc-pVDZ level. As for  $(\text{oP}^4)_3$ , heterochiral configurations of the macrocycle are predicted to be significantly more stable than homochiral configurations, by at least 3.8 kcal/mol. The most stable geometry is shown in Figure 5b. The *o*-phenylenes are well-accommodated by the macrocycle structure, with biaryl dihedrals along the *o*-phenylene backbone of approximately  $53^\circ$ , a close match to those of the parent hexa(*o*-phenylene) optimized at the same level of theory (also  $53^\circ$ ).<sup>[24]</sup>

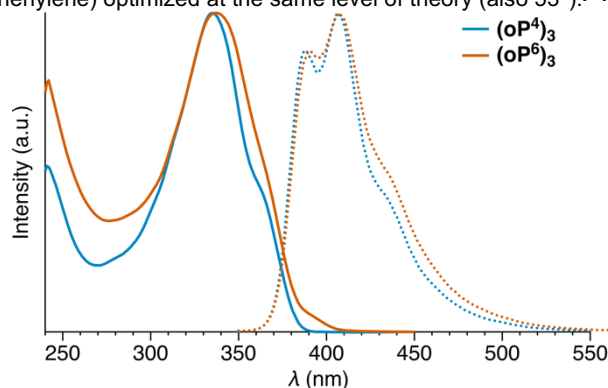


**Figure 6.** UV-vis (solid lines) and fluorescence (dotted lines) spectra of  $(\text{oP}^4)_3$  and  $(\text{oP}^6)_3$  in chloroform.

### Photophysics

UV-vis and fluorescence spectra of  $(\text{oP}^4)_3$  and  $(\text{oP}^6)_3$  are shown in Figure 6. In principle, these macrocycles are fully conjugated around their peripheries, with 42 and 54 electrons in the shortest conjugated paths around the rings. They are therefore both

## FULL PAPER

formally aromatic. However, folded *ortho*-phenylenes lack extended  $\pi$ -conjugation.<sup>[50,52]</sup> Consequently, the two macrocycles show similar photophysical properties despite the different oligomer lengths. Their UV-vis spectra are similar in shape, with maximum absorption wavelengths ( $\lambda_{\max}$ ) of 335 nm and 337 nm for (**oP<sup>4</sup>**)<sub>3</sub> and (**oP<sup>6</sup>**)<sub>3</sub>, respectively. These spectra are a close match to that of (*E*)-4,4'-diphenylstilbene ( $\lambda_{\max}$  = 342 nm),<sup>[59,60]</sup> which represents a single side of each macrocycle excluding conjugation through the *o*-phenylene moieties. Curiously, despite the structural and spectral similarities, the macrocycles show significantly different absorptivities ( $\epsilon$ ), with that of (**oP<sup>6</sup>**)<sub>3</sub> approximately double that of (**oP<sup>4</sup>**)<sub>3</sub> ( $(7.9 \pm 0.6) \times 10^4 \text{ M}^{-1}$  vs  $(3.8 \pm 0.3) \times 10^4 \text{ M}^{-1}$ ).

TD-DFT calculations at the CAM-B3LYP/6-311+G(2d,2p) level do a good job of matching the experimental spectra in terms of  $\lambda_{\max}$ , although the difference in  $\epsilon$  is not reproduced. The absorbance spectra for both macrocycles consist primarily of transitions to the first three excited states. In both cases, the orbitals contributing to these excited states are indeed primarily located on the 4,4'-diphenylstilbene moieties (Supporting Information).

The fluorescence spectra (Figure 6) are likewise similar and a good match to that of 4,4'-diphenylstilbene.<sup>[60]</sup> Both macrocycles are strongly fluorescent, with quantum yields of 0.88 and 0.81 for (**oP<sup>4</sup>**)<sub>3</sub> and (**oP<sup>6</sup>**)<sub>3</sub>, respectively (which are indistinguishable within experimental uncertainty). Fluorescence lifetimes were determined by time-correlated single photon counting. Both compounds gave good monoexponential fits with lifetimes of 1.4 ns and 1.1 ns for (**oP<sup>4</sup>**)<sub>3</sub> and (**oP<sup>6</sup>**)<sub>3</sub>.

## Conclusion

Twisted macrocycles (**oP<sup>4</sup>**)<sub>3</sub> and (**oP<sup>6</sup>**)<sub>3</sub> have been synthesized and characterized. Assembly by olefin metathesis is reasonably efficient, considering their sterically congested structures and the strain introduced on macrocyclization by the very short linkers. Characterization by NMR spectroscopy and X-ray crystallography shows that macrocycle (**oP<sup>4</sup>**)<sub>3</sub> favors a C<sub>2</sub>-symmetric, heterochiral geometry in both solution and the solid-state. DFT optimization confirms that this is indeed the most stable conformer for this system. Both X-ray crystallography and the DFT calculations show that the *o*-phenylene moieties are compressed in (**oP<sup>4</sup>**)<sub>3</sub>, indicating strain that may explain the relatively low yield. Similar behavior is observed for (**oP<sup>6</sup>**)<sub>3</sub>. The macrocycle predominantly adopts a heterochiral configuration of well-folded *o*-phenylene moieties, although misfolded states are observed by NMR spectroscopy. The photophysical properties of the two systems are very similar, with nearly identical absorbance and fluorescence spectra that can be assigned to 4,4'-diphenylstilbene chromophores, indicating that the twisted *o*-phenylenes break conjugation.

## Acknowledgements

CSH and VCK (synthesis, NMR spectroscopy, computational chemistry, photophysics) thank the National Science Foundation (CHE-1608213 and CHE-1904236) for support of this work and the Volwiler Distinguished Research Professorship. CJZ and BRS

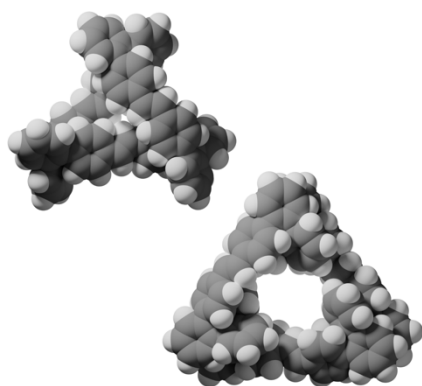
(crystallography) would like to acknowledge the University of Akron for support of this research.

**Keywords:** conformation analysis • hydrocarbons • chirality • foldamers • self-assembly

- [1] S. H. Gellman, *Acc. Chem. Res.* **1998**, *31*, 173–180.
- [2] G. Guichard, I. Huc, *Chem. Commun.* **2011**, *47*, 5933–5941.
- [3] D. J. Hill, M. J. Mio, R. B. Prince, T. S. Hughes, J. S. Moore, *Chem. Rev.* **2001**, *101*, 3893–4011.
- [4] I. Saraogi, A. D. Hamilton, *Chem. Soc. Rev.* **2009**, *38*, 1726–1743.
- [5] B. A. F. Le Bailly, J. Clayden, *Chem. Commun.* **2016**, *52*, 4852–4863.
- [6] G. Lautrette, B. Wicher, B. Kauffmann, Y. Ferrand, I. Huc, *J. Am. Chem. Soc.* **2016**, *138*, 10314–10322.
- [7] R. B. Prince, S. A. Barnes, J. S. Moore, *J. Am. Chem. Soc.* **2000**, *122*, 2758–2762.
- [8] J.-m. Suk, V. R. Naidu, X. Liu, M. S. Lah, K.-S. Jeong, *J. Am. Chem. Soc.* **2011**, *133*, 13938–13941.
- [9] Y. Hua, Y. Liu, C.-H. Chen, A. H. Flood, *J. Am. Chem. Soc.* **2013**, *135*, 14401–14412.
- [10] Z. C. Girvin, M. K. Andrews, X. Liu, S. H. Gellman, *Science* **2019**, *366*, 1528–1531.
- [11] D. Bécart, V. Diemer, A. Salaün, M. Oiarbide, Y. R. Nelli, B. Kauffmann, L. Fischer, C. Palomo, G. Guichard, *J. Am. Chem. Soc.* **2017**, *139*, 12524–12532.
- [12] A. Marcos Ramos, S. C. J. Meskers, E. H. A. Beckers, R. B. Prince, L. Brunsveld, R. A. J. Janssen, *J. Am. Chem. Soc.* **2004**, *126*, 9630–9644.
- [13] X. Li, N. Markandeya, G. Jonusauskas, N. D. McClenaghan, V. Maurizot, S. A. Denisov, I. Huc, *J. Am. Chem. Soc.* **2016**, *138*, 13568–13578.
- [14] S. P. Morcillo et al., *Chem. Sci.* **2016**, *7*, 5663–5670.
- [15] U. Lewandowska, W. Zajaczkowski, L. Chen, F. Bouillièrre, D. Wang, K. Koynov, W. Pisula, K. Müllen, H. Wennemers, *Angew. Chem., Int. Ed.* **2014**, *53*, 12537–12541.
- [16] J. S. Laursen, J. Engel-Andreasen, C. A. Olsen, *Acc. Chem. Res.* **2015**, *48*, 2696–2704.
- [17] C. M. Goodman, S. Choi, S. Shandler, W. F. DeGrado, *Nat. Chem. Biol.* **2007**, *3*, 252–262.
- [18] R. Gopalakrishnan, A. I. Frolov, L. Knerr, W. J. Drury III, E. Valeur, *J. Med. Chem.* **2016**, *59*, 9599–9621.
- [19] D. Mazzier, S. De, B. Wicher, V. Maurizot, I. Huc, *Angew. Chem., Int. Ed.* **2020**, *59*, 1606–1610.
- [20] D. Mazzier, S. De, B. Wicher, V. Maurizot, I. Huc, *Chem. Sci.* **2019**, *10*, 6984–6991.
- [21] S. De, B. Chi, T. Granier, T. Qi, V. Maurizot, I. Huc, *Nat. Chem.* **2018**, *10*, 51–57.
- [22] Z. J. Kinney, C. S. Hartley, *J. Am. Chem. Soc.* **2017**, *139*, 4821–4827.
- [23] Z. J. Kinney, C. S. Hartley, *Org. Lett.* **2018**, *20*, 3327–3331.
- [24] Z. J. Kinney, V. C. Kirinda, C. S. Hartley, *Chem. Sci.* **2019**, *10*, 9057–9068.
- [25] Z. Zhang, W.-Y. Cha, N. J. Williams, E. L. Rush, M. Ishida, V. M. Lynch, D. Kim, J. L. Sessler, *J. Am. Chem. Soc.* **2014**, *136*, 7591–7594.
- [26] B. Liu, C. G. Pappas, E. Zangrando, N. Demitri, P. J. Chmielewski, S. Otto, *J. Am. Chem. Soc.* **2019**, *141*, 1685–1689.
- [27] P. Reiné et al., *J. Org. Chem.* **2018**, *83*, 4455–4463.
- [28] K. Urushibara, Y. Ferrand, Z. Liu, H. Masu, V. Pophristic, A. Tanatani, I. Huc, *Angew. Chem., Int. Ed.* **2018**, *57*, 7888–7892.
- [29] R. Katoono, Y. Tanaka, K. Fujiwara, T. Suzuki, *J. Org. Chem.* **2014**, *79*, 10218–10225.
- [30] F. Chen, T. Tanaka, Y. Hong, W. Kim, D. Kim, A. Osuka, *Chem.—Eur. J.* **2016**, *22*, 10597–10606.
- [31] T. Hjelmggaard, L. Nauton, F. De Riccardis, L. Jouffret, S. Faure, *Org. Lett.* **2018**, *20*, 268–271.
- [32] M. Caricato, S. D. González, I. Arandia Ariño, D. Pasini, *Beilstein J. Org. Chem.* **2014**, *10*, 1308–1316.
- [33] M. Widhalm, P. Wimmer, G. Klitschar, *J. Organomet. Chem.* **1996**, *523*, 167–178.
- [34] S. Castro-Fernández, M. M. Cid, C. S. López, J. L. Alonso-Gómez, *J. Phys. Chem. A* **2015**, *119*, 1747–1753.

## FULL PAPER

- [35] P. Rivera-Fuentes, F. Diederich, *Angew. Chem., Int. Ed.* **2012**, *51*, 2818–2828.
- [36] G. R. Schaller, F. Topić, K. Rissanen, Y. Okamoto, J. Shen, R. Herges, *Nat. Chem.* **2014**, *6*, 608–613.
- [37] S. W. Sisco, J. S. Moore, *Chem. Sci.* **2014**, *5*, 81–85.
- [38] A. U. Malik, F. Gan, C. Shen, N. Yu, R. Wang, J. Crassous, M. Shu, H. Qiu, *J. Am. Chem. Soc.* **2018**, *140*, 2769–2772.
- [39] G. Naulet, L. Sturm, A. Robert, P. Dechambenoit, F. Röhricht, R. Herges, H. Bock, F. Durola, *Chem. Sci.* **2018**, *9*, 8930–8936.
- [40] C. S. Hartley, *Acc. Chem. Res.* **2016**, *49*, 646–654.
- [41] W. Zhang, J. S. Moore, *J. Am. Chem. Soc.* **2005**, *127*, 11863–11870.
- [42] C. W. Lee, R. H. Grubbs, *J. Org. Chem.* **2001**, *66*, 7155–7158.
- [43] Y. E. Bergman et al., *Org. Lett.* **2009**, *11*, 4438–4440.
- [44] O. M. Ogba, N. C. Warner, D. J. O'Leary, R. H. Grubbs, *Chem. Soc. Rev.* **2018**, *47*, 4510–4544.
- [45] Y. Jin, A. Zhang, Y. Huang, W. Zhang, *Chem. Commun.* **2010**, *46*, 8258–8260.
- [46] C. Yu, Y. Jin, W. Zhang, in *Dynamic Covalent Chemistry* (Eds.: W. Zhang, Y. Jin), John Wiley & Sons, Ltd, Chichester, UK, **2017**, pp. 121–163.
- [47] T. P. Money Penny II, N. P. Walter, Z. Cai, Y.-R. Miao, D. L. Gray, J. J. Hinman, S. Lee, Y. Zhang, J. S. Moore, *J. Am. Chem. Soc.* **2017**, *139*, 3259–3264.
- [48] H. Ding, R. Chen, C. Wang, in *Dynamic Covalent Chemistry* (Eds.: W. Zhang, Y. Jin), John Wiley & Sons, Ltd, Chichester, UK, **2017**, pp. 165–205.
- [49] X. Jiang, S. D. Laffoon, D. Chen, S. Pérez-Estrada, A. S. Danis, J. Rodríguez-López, M. A. Garcia-Garibay, J. Zhu, J. S. Moore, *J. Am. Chem. Soc.* **2020**, *142*, 6493–6498.
- [50] J. He, S. M. Mathew, S. D. Cornett, S. C. Grundy, C. S. Hartley, *Org. Biomol. Chem.* **2012**, *10*, 3398–3405.
- [51] S. M. Mathew, C. S. Hartley, *Macromolecules* **2011**, *44*, 8425–8432.
- [52] S. Ando, E. Ohta, A. Kosaka, D. Hashizume, H. Koshino, T. Fukushima, T. Aida, *J. Am. Chem. Soc.* **2012**, *134*, 11084–11087.
- [53] There is a small shoulder at higher retention time for the purified (**oP6**)<sub>3</sub>. We do not believe this represents a significant impurity as it is not present in the GPC traces of the crude mixtures. Regardless, the chromatogram demonstrates that the macrocycle can be separated from higher molecular weight species.
- [54] C. S. Hartley, E. L. Elliott, J. S. Moore, *J. Am. Chem. Soc.* **2007**, *129*, 4512–4513.
- [55] The separation of the oligomer termini can be ignored in the calculation of  $\beta$  as this does not affect the fit within the macrocycle.
- [56] CCDC 1996399-1996400 contain the supplementary crystallographic data for this paper. The data can be obtained free of charge from The Cambridge Crystallographic Data Centre via [www.ccdc.cam.ac.uk/structures](http://www.ccdc.cam.ac.uk/structures).
- [57] S. Mathew, L. A. Crandall, C. J. Ziegler, C. S. Hartley, *J. Am. Chem. Soc.* **2014**, *136*, 16666–16675.
- [58] For example, the small doublets from 5.85–6.15 ppm can be assigned to protons 2e or 3e in less-populated conformers.
- [59] Z. Fengqiang, J. Motoyoshiya, Y. Nishii, H. Aoyama, A. Kakehi, M. Shiro, *J. Photochem. Photobiol., A* **2006**, *184*, 44–49.
- [60] E. A. Andreeshchev, V. S. Viktorova, S. F. Kilin, Y. P. Kushakevich, I. M. Rozman, *Opt. Spektrosk.* **1968**, *24*, 387–390.

**Entry for the Table of Contents**

Macrocycles have been assembled from vinyl-substituted *ortho*-phenylenes using olefin metathesis. The major products are trimers with congested, twisted structures. Characterization by NMR spectroscopy, X-ray crystallography, and DFT calculations show that heterochiral configurations are favored. Photophysical properties are also discussed.

Key topic: Foldamer macrocycles

Institute and/or researcher Twitter usernames: @TheHartleyLab, @viraj\_chana